1996MNRAS.279..447R

Mon. Not. R. Astron. Soc. **279**, 447–458 (1996)

The metallicity distribution of G dwarfs in the solar neighbourhood

H. J. Rocha-Pinto and W. J. Maciel
Instituto Astronômico e Geofísico, Av. Miguel Stefano 4200, 04301-904 São Paulo, Brazil

Accepted 1995 October 4. Received 1995 September 15; in original form 1995 May 30

ABSTRACT

We derive a new metallicity distribution of G dwarfs in the solar neighbourhood, using *uvby* photometry and up-to-date parallaxes. Our distribution comprises 287 G dwarfs within 25 pc from the Sun, and differs considerably from the classic solar neighbourhood distribution of Pagel & Patchett and Pagel by having a prominent single peak around [Fe/H] = −0.20 dex. The raw data are corrected for observational errors and cosmic scatter assuming a deviation $\sigma = 0.1$. In order to obtain the true abundance distribution, we use the correction factors given by Sommer-Larsen, which take into account the stellar scale heights.

The distribution confirms the G dwarf problem, that is, the paucity of metal-poor stars relative to the predictions of the simple model of chemical evolution. Another feature of this distribution, which was already apparent in previous ones, is the small number of metal-rich stars again in comparison with the simple model. Our results indicate that it is very difficult to fit the simple model to this distribution, even with the definition of an 'effective yield'. A comparison with several models from the literature is made. We find that models with infall are the most appropriate to explain the new metallicity distribution. We also show that the metallicity distribution is compatible with a major era of star formation occurring 5 to 8 Gyr ago, similar to results found by several authors.

Key words: stars: abundances – stars: late-type – Galaxy: evolution – solar neighbourhood.

1 INTRODUCTION

The so-called G dwarf problem was established by van den Bergh (1962) and Schmidt (1963), and can be described as follows: the number of metal-poor stars in the solar vicinity is lower than would be expected on the basis of predictions of the simple model (see Tinsley 1980 for a review). Despite many theoretical efforts, this problem has remained, initially owing to the lack of successful models, and later owing to the multiplicity of them. In the earlier attempts to solve this problem, samples were very inhomogeneous, comprising stars of different spectral types compiled by several authors. More accurate data were obtained years later by Pagel & Patchett (1975), who established a non-biased sample of 132 G dwarfs within 25 pc of the Sun from the nearby star catalogues of Gliese (1969) and Woolley et al. (1970).

The use of only G dwarfs warrants the homogeneity of the sample, which can then be considered as representative of the chemical enrichment history of the Galaxy. In fact, G dwarfs are thought to have lifetimes greater than or equal to the age of our Galaxy, so that all stars of this type ever born in the Galaxy have not yet completed their evolutionary stages. Naturally, cooler stars have even longer lifetimes than G dwarfs. However, being less luminous, a sample based on K or M dwarfs would be confined to smaller regions, and thus more subject to biases.

A 'G dwarf problem' has not been found in the halo or in the bulge of the Galaxy (e.g., Beers, Preston & Schectman 1985; Laird et al. 1988; Geisler & Friel 1992), and it is not clear whether it exists for low-metallicity globular clusters, so that it may be connected with mechanisms operating mainly in the disc (Pagel 1987). Therefore, the metallicity distribution of the solar neighbourhood is a very important constraint to chemical evolution models for our Galaxy.

The metallicity distributions most often used in the literature are those of Pagel (1989) and Sommer-Larsen (1991). Pagel has revised previous data of Pagel & Patchett (1975) by means of a new calibration between the ultraviolet excess $\delta(U-B)$ and [Fe/H], and by using the oxygen abundance $\log\phi$ = [O/H] as a metallicity index. On the other hand, Sommer-Larsen (1991) applied a correction to the distribution of Pagel & Patchett, taking into account the fact that metal-poor stars are generally older and have larger scale heights than metal-rich stars.

The increasing sophistication in chemical evolution models (e.g., Sommer-Larsen & Yoshii 1990; Burkert, Truran & Hensler 1992; Pardi & Ferrini 1994; Carigi 1994) is supposed to be followed by an improvement of the database. Thus, it is desirable to have an up-to-date metallicity distribution comprising a larger number of G dwarfs, which could be used to discriminate more accurately among the different scenarios emerging from these models.

© 1996 RAS

© Royal Astronomical Society • Provided by the NASA Astrophysics Data System

1996MNRAS.279..447R

In this paper, we present a new metallicity distribution for the solar neighbourhood based on Strömgren photometry. In Section 2, we present a unbiased sample of G dwarfs from up-to-date photometric and parallax catalogues. In Section 3, we apply the corrections introduced by Pagel (1989) and Sommer-Larsen (1991) to the metallicity distribution. Some consequences for the chemical evolution of the Galaxy and our conclusions follow in Section 4.

2 SAMPLE SELECTION

2.1 Selection criteria

In order to obtain the G dwarf metallicity distribution, we followed the criteria of Pagel & Patchett (1975) for the selection of a non-biased sample of dwarfs. The stars were selected from the Third Catalogue of Nearby Stars (Gliese & Jahreiss 1991). We have taken all stars with spectral types between G0 V and G9 V. For stars with insufficient and/or ambiguous classification, we have selected those with visual absolute magnitude between 4.5 and $5.13+5.33(B-V)$, to exclude subgiants and white dwarfs, respectively (cf. Pagel & Patchett 1975). A few objects not classified as class V stars, but having absolute magnitudes in the interval above, were also selected. The total initial sample includes 345 stars.

We have taken *uvby* data from the catalogues of Olsen (1993) and Hauck & Mermilliod (1990). We have favoured the first catalogue, when a star appeared in both, because the catalogue of Hauck & Mermilliod lists average values from several previous works.

The number of stars of our initial sample that have photometric data in these catalogues is 293. Two of these stars (HD 206827 = HR 8310 and HD 218640 = HR 8817) have been excluded from our analysis in view of the following considerations. The first star is classified as G2V in Gliese & Jahreiss (1991) and in the Bright Star Catalogue, but is also referred to as an F dwarf (cf. Duquennoy & Mayor 1991). It has a close visual companion (HD 206826, F6V), and is also suspected of having a spectroscopic companion. It has a $b-y$ colour that is too low for a G dwarf ($b-y=0.241$), although it is compatible with that of an early F dwarf. The original paper (Oblak 1978) presents *uvby* colours for HD 206826 B, which Hauck & Mermilliod (1990) probably misassigned to HD 206827.

The second star, HD 218640, is classified as G2V (Gliese & Jahreiss 1991), but its absolute visual magnitude lies far beyond the magnitude range we have used to select our sample of G dwarfs. This star also has a close visual companion (HD 218641, A2V). The original reference (Olsen 1983) gives combined *uvby* colours for these stars, which were assigned by Hauck & Mermilliod to HD 218640 only.

2.2 Metallicity calibrations

The metallicity distributions obtained by Pagel & Patchett (1975) and Pagel (1989) were based on the *UBV* photometric system, which is not very good for the determination of accurate metallicities, since the relation between $\delta(U-B)$ and [Fe/H] is not very well defined. A metallicity distribution based on Strömgren photometry is likely to be less subject to errors. Olsen (1984) gives two calibrations in order to determine the metallicity:

$$[\mathrm{Fe/H}]_1 = -10\delta m_1 + 0.10 \tag{1}$$

and

$$[\mathrm{Fe/H}]_2 = -7.5\delta m_1 + 1.9\delta c_1 - 0.04, \tag{2}$$

where we have introduced

$$\delta m_1 = m_1^{\mathrm{Hyades}} - m_1^{\mathrm{star}} \tag{3}$$

and

$$\delta c_1 = c_1^{\mathrm{Hyades}} - c_1^{\mathrm{star}}. \tag{4}$$

Here m_1 and c_1 are the standard *uvby* indices. Equations (1) and (2) will be called first and second calibrations, respectively. The Hyades standard curves $m_1 \times (b-y)$ and $c_1 \times (b-y)$ for G dwarfs were taken from Crawford (1975) and Olsen (1984). The adopted sample is shown in Table 1, where we list the HD number (column 1), the spectral type (column 2), the photometric indices $(b-y)$ (column 3), m_1 (column 4), c_1 (column 5), δm_1 (column 6), and δc_1 (column 7). The metallicities as given by equations (1) and (2) are given in columns 8 and 9, respectively. The average errors derived from the metallicity calibration are in the range $0.15-0.17$ dex (cf. Olsen 1984).

A more recent metallicity calibration has been presented by Schuster & Nissen (1989), which makes use of the standard *uvby* indices themselves:

$$\begin{aligned}[\mathrm{Fe/H}]_3 = {} & 1.052 - 73.21m_1 + 280.9m_1(b-y) + \\ & 333.95m_1^2(b-y) - 595.5m_1(b-y)^2 + \\ & [5.486 - 41.62m_1 - 7.963(b-y)]\log(m_1 - c_3),\end{aligned} \tag{5a}$$

for $0.22 \leqslant (b-y) < 0.375$, and

$$\begin{aligned}[\mathrm{Fe/H}]_3 = {} & -2.0965 + 22.45m_1 - 53.8m_1^2 - \\ & 62.04m_1(b-y) + 145.5m_1^2(b-y) + \\ & [85.1m_1 - 13.8c_1 - 137.2m_1^2]c_1,\end{aligned} \tag{5b}$$

for $0.375 \leqslant (b-y) \leqslant 0.59$, which we shall call calibration 3. In equation (5a) we have introduced

$$c_3 = 0.6322 - 3.58(b-y) + 5.20(b-y)^2. \tag{6}$$

The average uncertainty for this calibration is $\simeq 0.16$ dex, and the metallicities derived are shown in column 10 of Table 1.

A comparison of $[\mathrm{Fe/H}]_1$ and $[\mathrm{Fe/H}]_3$ shows that calibration 1 yields smaller metallicities for the redder stars ($b-y \geqslant 0.45$) than calibration 3. This discrepancy may arise from the fact that equation (1) assumes a simple linear dependence of the metallicity on δm_1, which may be a poor approximation at lower metallicities (cf. Olsen 1984).

In Fig. 1, we compare the derived photometric abundances with spectroscopic abundances available in the literature for 79 stars of our sample. The spectroscopic metallicities $[\mathrm{Fe/H}]_S$ were taken from Edvardsson et al. (1993) and Cayrel de Strobel et al. (1992), and are shown in column 11 of Table 1. We have favoured the data from Edvardsson et al. for stars appearing in both works, as the values from Cayrel de Strobel et al. have been compiled from several different sources. Figs 1(a), 1(b) and 1(c) show the results of calibrations 1, 2 and 3, respectively. The dispersion is very large, but may be partially due to inhomogeneities of the catalogue of Cayrel de Strobel et al. (1992). It can be seen that calibrations 1 and 3 yield abundances in better agreement with the spectroscopic

© Royal Astronomical Society • Provided by the NASA Astrophysics Data System

1996MNRAS.279..447R

Table 1. *uvby* indices and abundances for a sample of G dwarfs.

HD	MK type	$b-y$	m_1	c_1	δm_1	δc_1	$[Fe/H]_1$	$[Fe/H]_2$	$[Fe/H]_3$	$[Fe/H]_S$
1237	G6 V	0.459	0.289	0.300	0.011	−0.061	−0.01	−0.24	−0.06	
1273	G2 V	0.410	0.184	0.250	0.046	0.019	−0.36	−0.35	−0.56	
1388	G2 V	0.379	0.191	0.345	0.014	−0.036	−0.04	−0.21	−0.01	
1461	G5 IV-V	0.421	0.244	0.360	−0.001	−0.102	0.11	−0.23	0.20	0.41
1835	G2 V	0.411	0.225	0.353	0.006	−0.085	0.04	−0.25	0.11	0.20
3405	G3 V	0.397	0.204	0.362	0.014	−0.077	−0.04	−0.29	0.03	
3443	G7 V	0.435	0.252	0.290	0.009	−0.043	0.01	−0.19	−0.11	−0.16
3795	G3 V	0.443	0.217	0.282	0.056	−0.039	−0.46	−0.53	−0.40	
3823	G1 V	0.364	0.150	0.349	0.047	−0.020	−0.37	−0.43	−0.48	
4208	G5 V	0.404	0.227	0.278	−0.003	−0.002	0.13	0.15	−0.09	
4307	G0 V	0.387	0.173	0.348	0.037	−0.050	−0.27	−0.41	−0.27	−0.28
4308	G3 V	0.409	0.187	0.302	0.042	−0.032	−0.32	−0.42	−0.35	−0.40
4614	G3 V	0.372	0.185	0.275	0.016	0.043	−0.06	0.02	−0.10	−0.31
4747	G9 V	0.460	0.295	0.275	0.007	−0.037	0.03	−0.16	−0.17	
5817	dG2	0.398	0.156	0.254	0.063	0.029	−0.53	−0.46	−0.71	
6582	G5 VI	0.434	0.199	0.215	0.061	0.033	−0.51	−0.43	−0.78	−0.90
6880	G8/K0 V	0.318	0.154	0.480	0.026	−0.096	−0.16	−0.42	−0.21	
9540	G8 V	0.451	0.291	0.294	−0.005	−0.054	0.15	−0.10	−0.03	
10145	G5 V	0.421	0.232	0.326	0.011	−0.068	−0.01	−0.25	0.02	
10700	G8 Vp	0.435	0.263	0.238	−0.002	0.009	0.12	0.13	−0.35	−0.58
10800	G2 V	0.392	0.195	0.303	0.019	−0.012	−0.09	−0.20	−0.16	
11112	G4 V	0.409	0.200	0.400	0.029	−0.130	−0.19	−0.51	−0.05	
11131	dG1	0.394	0.206	0.292	0.010	−0.003	0.00	−0.12	−0.12	−0.06
12051	dG7	0.475	0.309	0.372	0.021	−0.134	−0.11	−0.45	0.20	
12759	G3 V	0.433	0.227	0.333	0.031	−0.085	−0.21	−0.44	−0.08	
13043	G2 V	0.393	0.196	0.372	0.019	−0.082	−0.09	−0.34	−0.01	
13974	G0 Ve	0.386	0.191	0.254	0.018	0.045	−0.08	0.01	−0.33	−0.30
14412	G5 V	0.438	0.258	0.229	0.008	0.016	0.02	0.09	−0.44	
14802	G1 V	0.385	0.188	0.373	0.021	−0.072	−0.11	−0.33	−0.05	
15335	G0 V	0.387	0.160	0.370	0.050	−0.072	−0.40	−0.55	−0.43	−0.22
16397	G1 V	0.387	0.159	0.278	0.051	0.020	−0.41	−0.39	−0.55	
16623	G2 V-VI	0.372	0.152	0.372	0.049	−0.054	−0.39	−0.51	−0.50	
16784	G0 V	0.378	0.142	0.293	0.062	0.017	−0.52	−0.47	−0.67	
17169	G5 V	0.468	0.220	0.339	0.096	−0.101	−0.86	−0.96	−0.34	
18757	G4 V	0.413	0.199	0.303	0.035	−0.037	−0.25	−0.37	−0.26	
18803	G8 V	0.425	0.270	0.328	−0.022	−0.074	0.32	−0.01	0.20	
19034	dG5	0.416	0.214	0.263	0.023	−0.001	−0.13	−0.21	−0.32	
19467	G5 V	0.409	0.200	0.337	0.029	−0.067	−0.19	−0.39	−0.13	
20407	G3 V	0.373	0.162	0.280	0.039	0.037	−0.29	−0.26	−0.40	
20619	G1.5 V	0.405	0.214	0.269	0.011	0.006	−0.01	−0.11	−0.22	−0.45
20630	G5 Ve	0.415	0.242	0.310	−0.006	−0.047	0.16	0.24	0.06	0.04
20727	dG2	0.436	0.185	0.358	0.078	−0.112	−0.68	−0.83	−0.43	
20766	G2 V	0.404	0.196	0.289	0.028	−0.013	−0.18	−0.28	−0.27	−0.35
20794	G5 V	0.439	0.235	0.285	0.032	−0.040	−0.22	−0.36	−0.25	−0.54
20807	G2 V	0.383	0.177	0.297	0.030	0.006	−0.20	−0.26	−0.29	−0.23
21019	G2 V	0.449	0.203	0.298	0.080	−0.057	−0.70	−0.75	−0.48	
21411	G8 V	0.440	0.253	0.258	0.015	−0.014	−0.05	−0.18	−0.30	
24293	G5 V	0.412	0.211	0.332	0.022	−0.065	−0.12	−0.33	−0.07	
24365	G8 V	0.506	0.294	0.303	0.104	−0.062	−0.94	−0.94	−0.29	
24892	G8 V	0.461	0.240	0.313	0.063	−0.075	−0.53	−0.66	−0.24	
25680	G5 V	0.401	0.200	0.331	0.022	−0.051	−0.12	−0.30	−0.10	
26491	G3 V	0.406	0.188	0.329	0.038	−0.056	−0.28	−0.43	−0.25	−0.18
28255	G4 V	0.405	0.217	0.332	0.008	−0.057	0.02	−0.21	0.03	
29231	G8 V	0.469	0.307	0.327	0.011	−0.089	−0.01	−0.29	0.06	
30003	G5 V	0.427	0.230	0.339	0.020	−0.086	−0.10	−0.36	0.00	
30495	G1 V	0.395	0.207	0.326	0.009	−0.039	0.01	−0.18	−0.01	0.10
30649	G1 IV-V	0.384	0.155	0.293	0.053	0.009	−0.43	−0.42	−0.55	−0.51
32387	G8 V	0.501	0.247	0.291	0.140	−0.050	−1.30	−1.18	−0.55	
32778	G5 V	0.395	0.180	0.261	0.036	0.026	−0.26	−0.26	−0.45	
32923	G4 V	0.415	0.197	0.332	0.039	−0.069	−0.29	−0.46	−0.21	−0.20
33811	G8 IV-V	0.465	0.283	0.409	0.028	−0.171	−0.18	−0.57	0.25	
34101	G8 V	0.444	0.249	0.329	0.026	−0.087	−0.16	−0.40	−0.02	
34721	G0 V	0.361	0.174	0.364	0.021	−0.032	−0.11	−0.26	−0.17	
35956	G0 V	0.377	0.182	0.321	0.022	−0.009	−0.12	−0.22	−0.14	
36435	G5 Ve	0.454	0.300	0.263	−0.009	−0.024	0.19	0.21	−0.20	

© 1996

© Royal Astronomical Society • Provided by the NASA Astrophysics Data System

1996MNRAS.279..447R

Table 1 – *continued*

HD	MK type	$b-y$	m_1	c_1	δm_1	δc_1	$[Fe/H]_1$	$[Fe/H]_2$	$[Fe/H]_3$	$[Fe/H]_S$
37655	G0 V	0.380	0.176	0.373	0.029	−0.066	−0.19	−0.39	−0.17	
37706	G5 V	0.454	0.297	0.240	−0.006	−0.001	0.16	0.00	−0.35	
38858	G2 V	0.402	0.192	0.288	0.031	−0.010	−0.21	−0.29	−0.30	
39091	G1 V	0.370	0.190	0.367	0.010	−0.046	0.00	−0.20	−0.02	0.00
39587	G0 V	0.378	0.194	0.307	0.010	0.003	0.00	−0.11	−0.06	−0.03
41330	G0 V	0.389	0.161	0.348	0.051	−0.053	−0.41	−0.52	−0.44	−0.24
42250	dG7	0.469	0.287	0.333	0.031	−0.095	−0.21	−0.46	0.02	
42618	G4 V	0.403	0.216	0.303	0.007	−0.026	0.03	−0.15	−0.06	
42807	G2 V	0.418	0.226	0.289	0.013	−0.029	−0.03	−0.19	−0.14	
43162	G5 V	0.428	0.246	0.303	0.006	−0.051	0.04	−0.18	−0.03	
43834	G5 V	0.443	0.262	0.340	0.011	−0.097	−0.01	−0.31	0.10	0.01
44120	G3 V	0.378	0.174	0.408	0.030	−0.098	−0.20	−0.45	−0.18	
45184	G0 V	0.394	0.207	0.338	0.009	−0.049	0.01	−0.20	0.03	
48189	G0 V	0.392	0.195	0.309	0.019	−0.018	−0.09	−0.22	−0.14	
48938	G2 V	0.354	0.139	0.333	0.053	0.008	−0.43	−0.42	−0.55	−0.38
50692	G0 V	0.382	0.167	0.329	0.040	−0.024	−0.30	−0.38	−0.33	
51608	G7 V	0.461	0.297	0.325	0.006	−0.087	0.04	−0.25	0.07	
52711	G4 V	0.388	0.172	0.333	0.039	−0.036	−0.29	−0.40	−0.30	−0.15
53705	G3 V	0.396	0.173	0.331	0.044	−0.045	−0.34	−0.46	−0.35	
55575	G0 V	0.384	0.150	0.307	0.058	−0.005	−0.48	−0.49	−0.59	−0.28
56274	G2 V	0.396	0.148	0.266	0.069	0.020	−0.59	−0.52	−0.75	−0.70
59468	G5 IV-V	0.433	0.253	0.323	0.005	−0.075	0.05	−0.22	0.05	
59967	G4 V	0.399	0.200	0.301	0.020	−0.019	−0.10	−0.22	−0.17	
61994	dG5	0.445	0.247	0.298	0.029	−0.056	−0.19	−0.37	−0.16	
62613	G8 V	0.450	0.261	0.293	0.023	−0.053	−0.13	−0.31	−0.14	
63077	G0 V	0.371	0.137	0.278	0.063	0.042	−0.53	−0.43	−0.65	−0.78
64090	G2 VI	0.436	0.104	0.106	0.159	0.140	−1.49	−0.96	−1.84	−1.92
64184	G5 V	0.425	0.210	0.305	0.038	−0.051	−0.28	−0.42	−0.24	
64606	G8 V	0.454	0.211	0.208	0.080	0.031	−0.70	−0.58	−0.89	−0.99
65583	G8 V	0.455	0.220	0.229	0.073	0.010	−0.63	−0.57	−0.72	−0.60
65721	G6 V	0.453	0.248	0.268	0.041	−0.028	−0.31	−0.40	−0.35	
65907	G2 V	0.370	0.153	0.324	0.047	−0.003	−0.37	−0.40	−0.48	
67458	G4 IV-V	0.375	0.189	0.302	0.013	0.012	−0.03	−0.12	−0.10	
68017	G4 V	0.420	0.194	0.264	0.048	−0.005	−0.38	−0.41	−0.49	
69565	G8/K0 V	0.554	0.299	0.421	0.218	−0.197	−2.08	−2.05	−0.16	
69830	G7.5 V	0.457	0.297	0.314	−0.001	−0.075	0.11	−0.18	0.05	
70642	G6 V	0.435	0.252	0.350	0.009	−0.103	0.01	−0.30	0.13	
71148	G5 V	0.402	0.193	0.348	0.030	−0.070	−0.20	−0.39	−0.14	
71334	G4 V	0.415	0.210	0.324	0.026	−0.061	−0.16	−0.35	−0.12	
72905	G1 V	0.403	0.188	0.304	0.035	−0.027	−0.25	−0.36	−0.29	−0.08
73524	G4 IV-V	0.385	0.183	0.385	0.026	−0.084	−0.16	−0.39	−0.10	
73752	G3 V	0.447	0.277	0.394	0.002	−0.153	0.08	−0.35	0.30	
74842	G5 V	0.454	0.269	0.268	0.022	−0.029	−0.12	−0.26	−0.26	
75732	G8 V	0.536	0.357	0.415	0.115	−0.180	−1.05	−1.24	0.10	0.30
76151	G3 V	0.412	0.234	0.336	−0.001	−0.069	0.11	−0.16	0.12	0.01
77137	G5 V	0.437	0.233	0.365	0.031	−0.119	−0.21	−0.50	0.03	
78643	G1 V	0.368	0.166	0.385	0.033	−0.061	−0.23	−0.40	−0.32	
81809	G2 V	0.416	0.182	0.344	0.055	−0.082	−0.45	−0.61	−0.35	−0.31
82885	G8 V	0.473	0.304	0.372	0.022	−0.134	−0.12	−0.46	0.19	0.00
86728	G2 Va	0.416	0.234	0.388	0.003	−0.126	0.07	−0.30	0.22	0.10
88261	G3 V-VI	0.389	0.150	0.286	0.062	0.009	−0.52	−0.49	−0.65	
88725	G1 V	0.404	0.147	0.264	0.077	0.012	−0.67	−0.60	−0.82	
88742	G1 V	0.386	0.174	0.332	0.035	−0.033	−0.25	−0.37	−0.27	
89269	G5 V	0.420	0.208	0.292	0.034	−0.033	−0.24	−0.36	−0.27	
89906	dG2	0.422	0.208	0.253	0.036	0.004	−0.26	−0.30	−0.45	
90156	G5 V	0.424	0.208	0.296	0.038	−0.041	−0.28	−0.41	−0.28	
94340	G3/5 V	0.406	0.192	0.384	0.034	−0.111	−0.24	−0.51	−0.13	
94518	G2 V	0.382	0.174	0.277	0.033	0.028	−0.23	−0.23	−0.37	
95128	G0 V	0.392	0.203	0.337	0.011	−0.046	−0.01	−0.21	0.01	0.01
96700	G2 V	0.398	0.163	0.325	0.056	−0.042	−0.46	−0.54	−0.49	
97334	G0 V	0.392	0.210	0.311	0.004	−0.020	0.06	−0.11	−0.01	
97343	G8/K0 V	0.462	0.280	0.345	0.025	−0.107	−0.15	−0.43	0.08	
98230	G0 Ve	0.377	0.180	0.293	0.024	0.019	−0.14	−0.18	−0.23	−0.12
98281	G8 V	0.457	0.254	0.288	0.042	−0.049	−0.32	−0.45	−0.25	
100180	G0 V	0.373	0.174	0.353	0.027	−0.036	−0.17	−0.31	−0.26	

© Royal Astronomical Society • Provided by the NASA Astrophysics Data System

1996MNRAS.279..447R

Table 1 – *continued*

HD	MK type	$b-y$	m_1	c_1	δm_1	δc_1	$[Fe/H]_1$	$[Fe/H]_2$	$[Fe/H]_3$	$[Fe/H]_S$
101177	G0 V	0.371	0.182	0.310	0.018	0.010	−0.08	−0.16	−0.14	
101259	G6/8 V	0.508	0.229	0.315	0.174	−0.074	−1.64	−1.49	−0.61	
101501	G8 Ve	0.445	0.264	0.290	0.012	−0.048	−0.02	−0.22	−0.11	0.03
101563	G0 V	0.416	0.196	0.342	0.041	−0.080	−0.31	−0.50	−0.21	
102365	G5 V	0.418	0.199	0.278	0.040	−0.018	−0.30	−0.38	−0.38	−0.70
102438	G5 V	0.433	0.210	0.281	0.048	−0.033	−0.38	−0.46	−0.39	
102540	G5/6 V	0.469	0.227	0.312	0.091	−0.074	−0.81	−0.87	−0.38	
103095	G8 VI	0.482	0.224	0.166	0.121	0.073	−1.11	−0.81	−1.31	−1.40
103431	dG7	0.439	0.249	0.287	0.018	−0.042	−0.08	−0.26	−0.16	
103432	dG6	0.420	0.224	0.287	0.018	−0.028	−0.08	−0.23	−0.18	
103493	G5 V	0.401	0.194	0.288	0.028	−0.008	−0.18	−0.26	−0.27	
104471	G0 V	0.370	0.191	0.363	0.009	−0.042	0.01	−0.18	0.00	
105590	G2 V	0.420	0.220	0.320	0.022	−0.061	−0.12	−0.32	−0.08	−0.04
106116	G4 V	0.431	0.249	0.359	0.007	−0.109	0.03	−0.30	0.16	
106156	G8 V	0.471	0.329	0.341	−0.007	−0.103	0.17	−0.19	0.15	
108754	G8 V	0.435	0.217	0.237	0.044	0.010	−0.34	−0.35	−0.56	
108799	G0 V	0.381	0.174	0.319	0.032	−0.013	−0.22	−0.31	−0.26	
109358	G0 V	0.385	0.182	0.296	0.027	0.005	−0.17	−0.23	−0.25	−0.19
110010	dG2	0.395	0.228	0.387	−0.012	−0.100	0.22	−0.14	0.31	
110897	G0 V	0.374	0.149	0.284	0.053	0.032	−0.43	−0.38	−0.55	−0.59
111031	G5 V	0.426	0.250	0.376	−0.001	−0.123	0.11	−0.27	0.24	
111395	G7 V	0.438	0.241	0.334	0.025	−0.089	−0.15	−0.39	−0.01	
111515	G8 V	0.437	0.201	0.241	0.063	0.005	−0.53	−0.50	−0.65	
112164	G1 V	0.402	0.197	0.460	0.026	−0.182	−0.16	−0.58	−0.06	0.24
114260	G6 V	0.452	0.248	0.310	0.040	−0.070	−0.30	−0.47	−0.15	
114613	G3 V	0.441	0.235	0.390	0.035	−0.146	−0.25	−0.58	0.07	
114710	G0 V	0.370	0.191	0.337	0.009	−0.016	0.01	−0.13	0.00	0.03
115383	G0 V	0.376	0.191	0.383	0.012	−0.070	−0.02	−0.26	0.05	0.10
115617	G6 V	0.433	0.256	0.328	0.002	−0.080	0.08	−0.21	0.09	−0.03
116442	G5 V	0.467	0.310	0.251	0.005	−0.013	0.05	0.15	−0.32	
116443	G5 V	0.493	0.369	0.260	0.000	−0.020	0.10	0.18	−0.28	
117043	dG6	0.458	0.272	0.352	0.026	−0.113	−0.16	−0.45	0.10	
117176	G2.5 Va	0.451	0.221	0.354	0.065	−0.114	−0.55	−0.74	−0.19	−0.11
117635	G9 V	0.474	0.284	0.249	0.044	−0.011	−0.34	−0.39	−0.44	
117939	G4 V	0.424	0.191	0.303	0.055	−0.048	−0.45	−0.55	−0.40	
120690	G5 V	0.433	0.236	0.315	0.022	−0.067	−0.12	−0.33	−0.08	
121384	G8 V	0.482	0.234	0.302	0.111	−0.063	−1.01	−0.99	−0.46	
121849	G5 V	0.432	0.202	0.294	0.055	−0.045	−0.45	−0.54	−0.39	
122742	G8 V	0.452	0.264	0.317	0.024	−0.077	−0.14	−0.36	−0.03	
122862	G1 V	0.376	0.163	0.371	0.040	0.058	−0.30	−0.45	−0.32	
123505	G9 V	0.475	0.255	0.234	0.075	0.004	−0.65	−0.60	−0.66	
124580	G4 V	0.384	0.177	0.314	0.031	−0.012	−0.21	−0.30	−0.26	
125184	G8 V	0.454	0.247	0.413	0.044	−0.174	−0.34	−0.70	0.11	0.13
126053	G1 V	0.406	0.183	0.287	0.043	−0.014	−0.33	−0.39	−0.41	
126525	G5 V	0.426	0.222	0.310	0.027	−0.057	−0.17	−0.35	−0.14	
127334	G5 V	0.441	0.245	0.366	0.025	−0.122	−0.15	−0.46	0.09	0.05
127356	G5 V	0.448	0.217	0.261	0.064	−0.020	−0.54	−0.56	−0.53	
128400	G5 V	0.438	0.243	0.306	0.023	−0.061	−0.13	−0.32	−0.10	
128620	G2 V	0.438	0.248	0.373	0.018	−0.128	−0.08	−0.41	0.15	0.15
129333	dG0	0.408	0.202	0.301	0.026	−0.030	−0.16	−0.29	−0.21	
130307	G8 V	0.521	0.405	0.275	0.030	−0.035	−0.20	−0.33	−0.24	
130948	G2 V	0.383	0.179	0.326	0.028	−0.023	−0.18	−0.30	−0.20	0.20
131923	G5 V	0.443	0.228	0.361	0.045	−0.118	−0.35	−0.60	−0.06	
134319	dG5	0.419	0.222	0.276	0.018	−0.017	−0.08	−0.21	−0.23	
134987	G5 V	0.434	0.256	0.375	0.004	−0.127	0.06	−0.31	0.23	
135101	G5 V	0.436	0.217	0.369	0.046	−0.123	−0.36	−0.62	−0.09	
135101	G7 V	0.460	0.251	0.353	0.051	−0.115	−0.41	−0.64	−0.03	
136352	G2 V	0.409	0.181	0.298	0.048	−0.028	−0.38	−0.46	−0.41	−0.40
137107	G2 V	0.369	0.185	0.341	0.014	−0.019	−0.04	−0.18	−0.08	
137392	G1 V	0.383	0.196	0.370	0.011	−0.067	−0.01	−0.25	0.05	0.05
137676	G5 V	0.476	0.226	0.293	0.106	−0.055	−0.96	−0.94	−0.51	
140538	G5 V	0.425	0.228	0.336	0.020	−0.082	−0.10	−0.34	−0.01	
140901	G6 V	0.436	0.268	0.324	−0.005	−0.078	0.15	−0.15	0.11	
141004	G0 V	0.385	0.199	0.354	0.010	−0.053	0.00	−0.21	0.05	−0.04
141272	G8 V	0.479	0.324	0.304	0.014	−0.065	−0.04	−0.27	−0.05	

© 199

© Royal Astronomical Society • Provided by the NASA Astrophysics Data System

1996MNRAS.279..447R

Table 1 – *continued*

HD	MK type	$b-y$	m_1	c_1	δm_1	δc_1	$[Fe/H]_1$	$[Fe/H]_2$	$[Fe/H]_3$	$[Fe/H]_S$
142267	G1 V	0.393	0.159	0.276	0.056	0.014	−0.46	−0.43	−0.59	−0.28
143761	G2 V	0.394	0.183	0.322	0.033	−0.033	−0.23	−0.35	−0.24	−0.26
144009	G8 V	0.450	0.251	0.327	0.033	−0.087	−0.23	−0.45	−0.05	
144087	G8 V	0.450	0.265	0.338	0.019	−0.098	−0.09	−0.37	0.06	
144179	G9 V	0.481	0.308	0.254	0.035	−0.015	−0.25	−0.33	−0.38	
144287	G8 V	0.470	0.270	0.325	0.050	−0.087	−0.40	−0.58	−0.09	
144579	G8 V	0.455	0.232	0.226	0.061	0.013	−0.51	−0.47	−0.68	
145809	G3 V	0.396	0.187	0.328	0.030	−0.042	−0.20	−0.35	−0.20	
146233	G1 V	0.405	0.211	0.345	0.014	−0.070	−0.04	−0.28	0.01	0.02
146775	G0 V	0.379	0.211	0.318	−0.006	−0.009	0.16	0.17	0.11	
147231	dG5	0.443	0.217	0.328	0.056	−0.085	−0.46	−0.62	−0.23	
147513	G3/5 V	0.400	0.198	0.324	0.023	−0.043	−0.13	−0.29	−0.12	
147584	G0 V	0.352	0.177	0.323	0.014	0.020	−0.04	−0.11	−0.06	−0.15
149414	G5 Ve	0.472	0.202	0.155	0.122	0.083	−1.12	−0.80	−1.40	−1.14
150433	dG2	0.410	0.173	0.313	0.057	−0.044	−0.47	−0.55	−0.47	
150474	G8 V	0.477	0.261	0.364	0.073	−0.125	−0.63	−0.83	−0.04	
150706	dG3	0.389	0.188	0.312	0.024	−0.017	−0.14	−0.25	−0.18	
152391	G8 V	0.456	0.285	0.298	0.009	−0.059	0.01	−0.22	−0.06	
153631	G2 V	0.386	0.189	0.339	0.020	−0.040	−0.10	−0.27	−0.09	
154088	G8 IV-V	0.514	0.306	0.425	0.112	−0.184	−1.02	−1.23	0.10	
154345	G8 V	0.452	0.261	0.285	0.027	−0.045	−0.17	−0.33	−0.20	
155918	G2 V	0.391	0.144	0.277	0.069	0.016	−0.59	−0.53	−0.75	
156274	G8 V	0.482	0.291	0.259	0.054	−0.020	−0.44	−0.48	−0.40	
156365	G3 V	0.418	0.230	0.406	0.009	−0.146	0.01	−0.39	0.20	
156826	G9 V	0.519	0.296	0.327	0.134	−0.087	−1.24	−1.21	−0.25	
157214	G2 V	0.409	0.182	0.309	0.047	−0.039	−0.37	−0.47	−0.38	−0.41
159222	G5 V	0.408	0.212	0.365	0.016	−0.094	−0.06	−0.34	0.04	
159656	G5 V	0.412	0.199	0.352	0.034	−0.085	−0.24	−0.45	−0.13	
159704	G8 V	0.469	0.269	0.322	0.049	−0.084	−0.39	−0.57	−0.10	
159868	G5 V	0.451	0.219	0.356	0.067	−0.116	−0.57	−0.76	−0.20	
160269	G0 Va	0.399	0.184	0.327	0.036	−0.045	−0.26	−0.39	−0.25	
160691	G5 V	0.432	0.244	0.395	0.013	−0.146	−0.03	−0.41	0.20	0.16
161612	G8 V	0.447	0.246	0.375	0.033	−0.134	−0.23	−0.54	0.08	
163840	G2 V	0.406	0.220	0.357	0.006	−0.084	0.04	−0.25	0.11	
165185	G5 V	0.388	0.180	0.315	0.031	−0.018	−0.21	−0.31	−0.25	
165401	G2 V	0.393	0.164	0.287	0.051	0.003	−0.41	−0.42	−0.51	−0.46
168009	G2 V	0.411	0.199	0.351	0.032	−0.083	−0.22	−0.44	−0.13	
168060	G5 V	0.463	0.267	0.396	0.040	−0.158	−0.30	−0.64	0.16	
168443	G8 V	0.455	0.233	0.377	0.060	−0.138	−0.50	−0.75	−0.06	
171067	G8 V	0.424	0.234	0.309	0.012	−0.054	−0.02	−0.24	−0.05	
171665	G5 V	0.420	0.230	0.309	0.012	−0.050	−0.02	−0.22	−0.05	
172051	G5 V	0.418	0.216	0.277	0.023	−0.017	−0.13	−0.25	−0.26	
175541	G8 V	0.564	0.294	0.413	0.248	−0.197	−2.38	−2.27	−0.26	
176377	G2 V	0.385	0.181	0.291	0.028	0.010	−0.18	−0.23	−0.28	
176982	dG5	0.463	0.224	0.348	0.083	−0.110	−0.73	−0.87	−0.25	
178428	G5 V	0.438	0.246	0.354	0.020	−0.109	−0.10	−0.39	0.08	
181321	G5 V	0.400	0.192	0.302	0.029	−0.021	−0.19	−0.30	−0.24	
181655	G8 V	0.420	0.234	0.322	0.008	−0.063	0.02	−0.22	0.02	
185454	G5 V	0.427	0.273	0.309	−0.023	−0.056	0.33	0.02	0.12	
186408	G2 V	0.410	0.214	0.375	0.016	−0.106	−0.06	−0.36	0.06	0.21
186427	G5 V	0.416	0.226	0.354	0.011	−0.092	−0.01	−0.30	0.09	0.10
187923	G0 V	0.415	0.192	0.342	0.044	−0.079	−0.34	−0.52	−0.24	0.06
189340	G0 V	0.371	0.194	0.328	0.006	−0.008	0.04	−0.10	0.03	
189567	G2 V	0.406	0.185	0.297	0.041	−0.024	−0.31	−0.40	−0.36	−0.30
190067	G8 V	0.452	0.233	0.287	0.055	−0.047	−0.45	−0.54	−0.33	
190248	G8 V	0.458	0.310	0.366	−0.012	−0.127	0.22	−0.19	0.27	0.30
190360	G8 IV-V	0.461	0.275	0.372	0.028	−0.134	−0.18	−0.51	0.15	0.26
190406	G1 V	0.387	0.187	0.347	0.023	−0.049	−0.13	−0.31	−0.10	
192020	G8 V	0.500	0.393	0.280	−0.009	−0.039	0.19	0.24	−0.19	
193664	G5 V	0.379	0.176	0.330	0.029	−0.021	−0.19	−0.30	−0.20	0.06
194640	G5 V	0.440	0.274	0.301	−0.006	−0.057	0.16	−0.11	0.01	
195987	G9 V	0.479	0.292	0.271	0.046	−0.032	−0.36	−0.45	−0.31	
196761	G8 V	0.440	0.251	0.269	0.017	−0.025	−0.07	−0.22	−0.25	
196850	G2 V	0.396	0.194	0.328	0.023	−0.042	−0.13	−0.29	−0.13	
197076	G5 V	0.397	0.189	0.325	0.029	−0.040	−0.19	−0.33	−0.19	

© Royal Astronomical Society • Provided by the NASA Astrophysics Data System

1996MNRAS.279..447R

Table 1 – *continued*

HD	MK type	$b-y$	m_1	c_1	δm_1	δc_1	$[Fe/H]_1$	$[Fe/H]_2$	$[Fe/H]_3$	$[Fe/H]_S$
197214	G5 V	0.423	0.217	0.250	0.028	0.006	−0.18	−0.24	−0.42	
199288	G0 V	0.385	0.146	0.266	0.063	0.035	−0.53	−0.44	−0.71	
202457	G5 V	0.432	0.221	0.368	0.036	−0.119	−0.26	−0.54	−0.03	
202573	G5 V	0.567	0.237	0.479	0.312	−0.266	−3.02	−2.89	−0.70	
202628	G5 V	0.404	0.198	0.319	0.026	−0.043	−0.16	−0.32	−0.16	
202940	G5 V	0.450	0.247	0.273	0.037	−0.033	−0.27	−0.38	−0.31	
203244	G5 V	0.444	0.250	0.264	0.025	−0.022	−0.15	−0.27	−0.30	
205905	G4 IV-V	0.388	0.219	0.329	−0.008	−0.032	0.18	0.22	0.15	
206827	G2 V	0.241	0.148	0.520	−0.029	0.967	***	***	***	
206860	G0 V	0.376	0.186	0.318	0.017	−0.005	−0.07	−0.18	−0.10	
207129	G2 V	0.386	0.181	0.340	0.028	−0.041	−0.18	−0.33	−0.18	
210460	G0 V	0.451	0.208	0.328	0.078	−0.088	−0.68	−0.79	−0.36	
210918	G5 V	0.415	0.195	0.323	0.041	−0.060	−0.31	−0.46	−0.25	
211038	G8 V	0.556	0.290	0.433	0.232	−0.210	−2.22	−2.18	−0.21	
211415	G1 V	0.386	0.187	0.292	0.022	0.007	−0.12	−0.19	−0.22	
211998	G0 V	0.447	0.116	0.240	0.163	0.001	−1.53	−1.26	−1.43	−1.61
212330	G4 V	0.424	0.206	0.364	0.040	−0.109	−0.30	−0.55	−0.12	−0.17
212697	G3 V	0.392	0.204	0.284	0.010	0.007	0.00	−0.10	−0.15	0.30
213628	G3 V	0.441	0.266	0.315	0.004	−0.071	0.06	−0.21	0.03	
213941	G5 V	0.416	0.196	0.283	0.041	−0.021	−0.31	−0.39	−0.37	
214615	G8/K0 V	0.469	0.306	0.301	0.012	−0.063	−0.02	−0.25	−0.06	
214953	G1 V	0.362	0.171	0.379	0.025	−0.048	−0.15	−0.32	−0.21	
217014	G4 V	0.416	0.232	0.364	0.005	−0.102	0.05	−0.27	0.16	0.06
218209	G6 V	0.419	0.189	0.258	0.051	0.001	−0.41	−0.42	−0.54	
218640	G2 V	0.418	0.209	0.744	0.030	−0.484	***	***	***	
219048	G5 V	0.457	0.229	0.329	0.067	−0.090	−0.57	−0.72	−0.23	
219709	G2 V	0.395	0.210	0.336	0.006	−0.049	0.04	−0.18	0.05	
221818	G8 V	0.469	0.297	0.286	0.021	−0.048	−0.11	−0.29	−0.16	
223498	G7 V	0.456	0.272	0.366	0.022	−0.127	−0.12	−0.45	0.15	
224465	dG2	0.415	0.224	0.338	0.012	−0.075	−0.02	−0.27	0.04	
224930	G3 V	0.428	0.189	0.215	0.063	0.037	−0.53	−0.44	−0.80	−0.70
225239	G2 V	0.412	0.169	0.312	0.064	−0.045	−0.54	−0.60	−0.53	−0.50
225261	G9 V	0.453	0.271	0.252	0.018	−0.012	−0.08	−0.20	−0.34	

ıbundances than calibration 2. The agreement is better for calbration 3, so that we will adopt the photometric abundances ıs given by equations (5).

².3 Halo contamination

)ur sample may include some halo stars. To exclude them, we ntroduced a *chemical* criterion, according to which all stars ıaving [Fe/H] < −1.2 are considered to be halo members. The ıpplication of this condition to the objects of Table 1 excludes our stars, so that our final sample contains 287 objects.

A *kinematical* criterion was also considered, namely, objects having radial velocities $|v_r|$ or tangential velocities $|v_t|$ arger than 100 km s^{-1} are likely to be halo members. This riterion tends to remove objects with large velocity compoıents, a characteristic generally shared by halo stars. However, t should be recalled that our sample comprises stars within ²5 pc from the Sun only. Since parallaxes are preferentially neasured in stars with large proper motions, large velocity omponents could be obtained even for disc stars, owing to heir proximity. In fact, using radial velocities from Gliese ⁄ Jahreiss (1991), and calculating tangential velocities from ›roper motions and parallaxes of the same source, we find that 9 stars should be excluded from our initial sample, accordng to the kinematical criterion. The four objects excluded on he basis of the chemical criterion also belong to this group, vhich reinforces the suspicion that they are halo members. The remaining 15 objects have disc metallicities. Since the resulting metallicity distribution is not affected by the kinematical criterion, we have decided to take into account the chemical criterion only.

2.4 Metal content and lifetimes of the hotter G dwarfs

The relative metallicity distribution of our adopted sample is shown in Fig. 2 (continuous line), and the corresponding data are given in Table 2. In this table, column 1 gives the adopted metallicity intervals, and column 3 gives the raw absolute distribution, which we will call ΔN_0.

A remark should be made with respect to the spectral types considered. Pagel & Patchett (1975) used only stars with spectral types between G2 V and G8 V. Earlier stars, with spectral types G0 V and G1 V, were not used, since their lifetimes are considered as slightly lower than the assumed age of the Galaxy. On the other hand, G9 V stars were not included, as their low effective temperatures invalidate their adopted calibration. The latter problem does not occur with our adopted calibrations, so that we have included G9 V stars in our sample.

Data selection based on a given spectral range has some limitations, in the sense that the spectral types depend both on the effective temperature and on the metal content. Moreover, the stellar chemical composition also affects its lifetime.

The effect of differing metal content would be a modifica-

© Royal Astronomical Society • Provided by the NASA Astrophysics Data System

1996MNRAS.279..447R

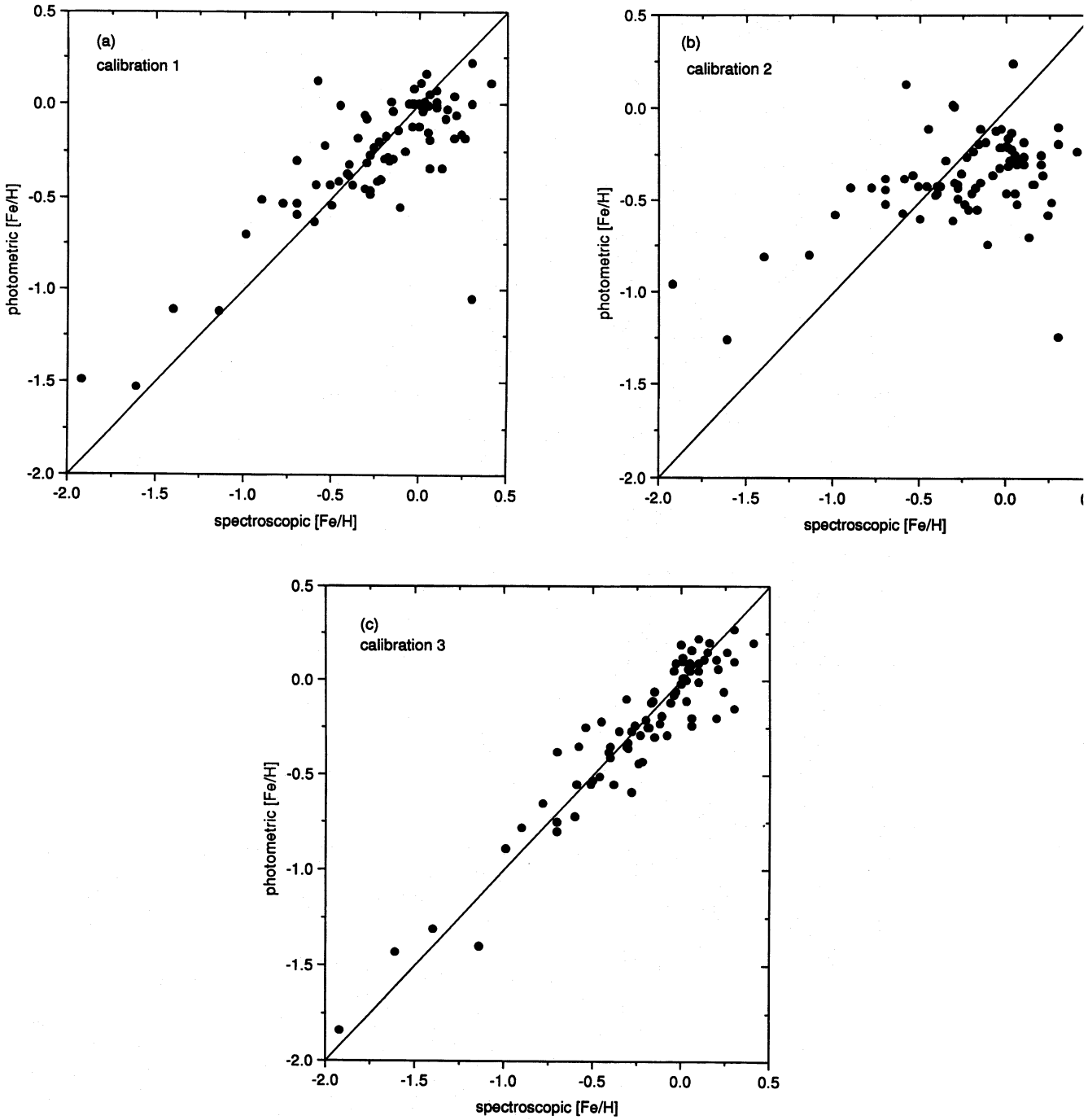

Figure 1. Photometric versus spectroscopic abundances for 79 stars of our sample. (a) Calibration 1 (equation 1); (b) calibration 2 (equation 2) (c) calibration 3 (equations 5).

tion of the mass range of the stars classified as G dwarfs, which would affect the homogeneity of our sample. In this case, the G dwarf metallicity distribution would differ from the corresponding distribution of the long-lived stars for which the theoretical results apply. On the other hand, the effect of the chemical composition on the lifetimes could also produce a 'G dwarf problem' (Bazan & Mathews 1990; Meusinger & Stecklum 1992), as metal-poor stars have lower lifetimes, and some of them may have already died. However, the magnitudes of these effects are not at all clear, partly because they are strongly dependent on stellar evolution models.

In order to check the effects of the hotter stars, we plotte in Fig. 2 the metallicity distribution of the 231 objects wit spectral types between G2 and G9 V (squares). As can b seen from the figure, the plotted distributions are very similar suggesting that the inclusion of the earlier stars does not imply a biased sample. This conclusion is reinforced by Fig. 3, where we plot the metallicity of each star (dots), along with the mean value for each spectral type (squares). Here, G8 and G9 stars are merged in the same bin. Since G0 and G1 V stars are hotter and have shorter lifetimes, we would expect their metallicity to be larger than for the remaining, cooler stars

© Royal Astronomical Society • Provided by the NASA Astrophysics Data System

1996MNRAS.279..447R

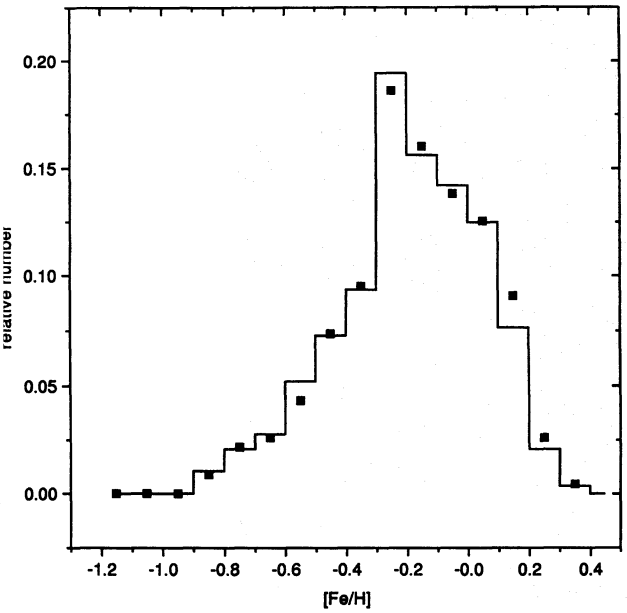

Figure 2. Metallicity distribution of 287 dwarf stars with spectral types in the range G0 – G9 (continuous line), and 231 dwarfs of spectral types G2 – G9 (squares).

We see that there is a good agreement of the metallicity of G0 and G1 stars with the average values of the remaining spectral types. Also, the scatter around the mean value is similar for all spectral types, except types G6 and G7, for which there are fewer stars. Therefore, we believe that there is no reason to exclude such objects from our sample, which comprises then 287 stars with spectral types in the range G0 – G9 V.

3 ADDITIONAL CORRECTIONS

Following Pagel & Patchett (1975) and Pagel (1989), we have corrected the final distribution for observational errors and cosmic scatter in the age–metallicity relation, assuming a standard deviation of 0.1 dex. For purposes of deconvolution, the raw distribution in column 3 of Table 1 was fitted to a Gaussian given by $(A/\sigma\sqrt{2\pi})\exp[-([\mathrm{Fe/H}]-\mu)^2/2\sigma^2]$, where $A = 28.48, \mu = -0.16$, and $\sigma = 0.23$. The deconvolved Gaussian has $\sigma = 0.21$; the corrections $\delta(\Delta N)_0$ are obtained by the subtraction of the first Gaussian from its deconvolved version, and are given in the fourth column of Table 2. We have also considered a standard deviation $\sigma = 0.15$ dex, which is of the order of the error estimated for calibration 1. In this case, the final distribution does not appreciably change in comparison with the results presented in Table 2.

We have also made use of the oxygen abundance rather than the iron abundance, in order to be consistent with chemical evolution models that use the instantaneous recycling approximation. We adopt the same [O/Fe] ratio as given by Pagel (1989):

$$\log\phi = [\mathrm{O/H}] = 0.5[\mathrm{Fe/H}]. \qquad (7)$$

The oxygen abundances ϕ are given in the second column of Table 2.

As in Pagel (1989), our distribution is spatially limited within 25 pc of the Sun, which may introduce a non-negligible bias in the metallicity distribution, as was shown by Sommer-Larsen (1991). Since older stars generally have lower metallicities and larger scale heights relative to the galactic plane, we expect their relative number to be artificially reduced by the limitation of our sample within 25 pc of the Sun. To solve this problem, we have adopted the correction procedure introduced by Sommer-Larsen (1991), who defined a weight factor f, which is given in column 5 of Table 2. This factor has been determined by Sommer-Larsen (1991) on the basis of kinematical models by Norris & Ryan (1989) and Kuijken & Gilmore (1989). According to Sommer-Larsen (1991), f is essentially independent of the specific model parameters, so that we adopted the values obtained for the models by Kuijken & Gilmore (1989) which reproduce the rotation curve and surface density in a maximum disc type model (cf. Sellwood & Sanders 1988). Following Sommer-Larsen (1991), we have applied the correction factors f^{-1} to the *raw data* as given in column 3 of Table 2, and again fitted a Gaussian to the resulting distribution, for which we obtained $A = 31.95, \mu = -0.19$, and $\sigma = 0.27$. This was also deconvolved to correct for observational errors and cosmic scatter assuming a deviation of 0.1. The calculated deviation becomes $\sigma = 0.26$, and the new correction factors, which we denote as $\delta(\Delta N)_1$, are determined as before, and given in column 6 of Table 2.

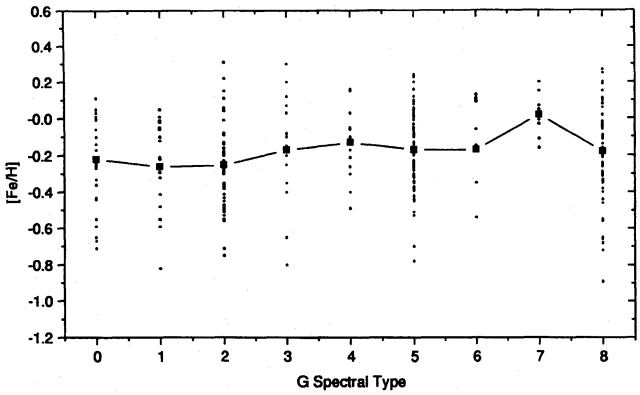

Figure 3. Abundances as a function of the spectral type (dots), and mean values for each type (squares). Stars of types G8 and G9 are merged in the same bin.

The obtained relative distributions are given in the last two columns of Table 2. Column 7 gives the raw distribution corrected for observational errors and cosmic scatter *only*, and column 8 gives the final distribution, which also includes the scale height correction according to Sommer-Larsen (1991). In these columns, the first four bins were grouped to yield a mean value for the distribution. This procedure was also used for the last two bins.

4 CONSEQUENCES FOR CHEMICAL EVOLUTION

Fig. 4 shows our raw relative distribution $\Delta N_0/287$ (thick continuous line) as a function of the metallicity in comparison with the equivalent quantity from Pagel, $\Delta N/132$ (broken line, cf. Pagel 1989, p. 210). Also shown is the metallicity distribution of Rana & Basu (1990, thin line). It can be seen that our distribution presents a single, main peak located between the main peaks of the previously quoted distributions. Our distribution is narrower than the one by Pagel (1989), and has

© Royal Astronomical Society • Provided by the NASA Astrophysics Data System

1996MNRAS.279..447R

Table 2. Abundance distribution in the solar neighbourhood.

[Fe/H]	ϕ	ΔN_0	$\delta(\Delta N)_0$	f	$\delta(\Delta N)_1$	$\log\left[\frac{\Delta N_0+\delta(\Delta N)_0}{\Delta\phi}\right]$	$\log\left[\frac{\Delta N_0/f+\delta(\Delta N)_1}{\Delta\phi}\right]$
−1.2 to −1.1	0.25 to 0.28	0	0.00	0.23	−0.06		
−1.1 to −1.0	0.28 to 0.32	0	−0.03	0.23	−0.17	1.22(+0.21, −0.43)	1.89(+0.11, −0.15)
−1.0 to −0.9	0.32 to 0.35	0	−0.11	0.23	−0.40		
−0.9 to −0.8	0.35 to 0.40	3	−0.36	0.23	−0.80		
−0.8 to −0.7	0.40 to 0.45	6	−0.92	0.36	−1.27	2.01(+0.16, −0.25)	2.49(+0.10, −0.13)
−0.7 to −0.6	0.45 to 0.50	8	−1.78	0.53	−1.54	2.09(+0.15, −0.22)	2.43(+0.10, −0.14)
−0.6 to −0.5	0.50 to 0.56	15	−2.37	0.79	−1.17	2.32(+0.11, −0.14)	2.47(+0.09, −0.12)
−0.5 to −0.4	0.56 to 0.63	21	−1.61	0.85	0.07	2.44(+0.09, −0.11)	2.55(+0.08, −0.10)
−0.4 to −0.3	0.63 to 0.71	27	1.01	0.98	1.82	2.54(+0.08, −0.09)	2.56(+0.07, −0.09)
−0.3 to −0.2	0.71 to 0.79	56	4.14	0.99	3.19	2.88(+0.05, −0.06)	2.87(+0.05, −0.06)
−0.2 to −0.1	0.79 to 0.89	45	5.31	1.00	3.33	2.70(+0.06, −0.07)	2.68(+0.06, −0.07)
−0.1 to 0.0	0.89 to 1.00	41	3.45	1.00	2.16	2.61(+0.06, −0.07)	2.59(+0.06, −0.07)
0.0 to 0.1	1.00 to 1.12	36	0.22	1.00	0.40	2.48(+0.07, −0.08)	2.48(+0.07, −0.08)
0.1 to 0.2	1.12 to 1.26	22	−1.98	1.00	−0.99	2.16(+0.09, −0.11)	2.18(+0.09, −0.11)
0.2 to 0.3	1.26 to 1.41	6	−2.30	1.00	−1.53	0.99(+0.19, −0.36)	1.11(+0.17, −0.30)
0.3 to 0.4	1.41 to 1.58	1	−1.56	1.00	−1.36		

a prominent peak around −0.20 dex, and is in this respect similar to the distribution by Rana & Basu (1990). However, our distribution does not confirm the large number of stars with [Fe/H] > 0.1 dex found by these authors. Instead, it shows a small percentage of these stars, similar to that found by Pagel.

A remarkable feature of our distribution is that it shows no stars in the interval $-1.2 \leqslant$ [Fe/H] $\leqslant -0.8$. This does not mean that such stars do not exist (a metallicity distribution based on calibration 1, for instance, shows 12 stars in this range), but that their number is small. This result not only confirms the G dwarf problem, but aggravates it, in comparison with previous distributions at this metallicity range.

Another feature of our distribution is the strong peak observed, which could be interpreted as the result of a star formation burst. To illustrate this, let us assume that the age of a star can be determined on the basis of an age–metallicity relation (AMR). Of course, there is a large scatter in this relation (cf. Edvardsson et al. 1993), so that this should be considered for illustration purposes only. Adopting the parametrization of the AMR given by Rana (1991), we have

$$[\mathrm{Fe/H}] = 0.68 - \frac{11.2}{8+t}, \qquad (8)$$

where t is the age, taken as $t = 0$ at the birth of the disc, and $t = 12$ Gyr for the disc age. Assuming that the burst occurred in the range $-0.10 \leqslant$ [Fe/H] $\leqslant -0.30$, it can be concluded that it occurred some 5 to 8 Gyr ago, similar to the results found by other authors on the basis of different methods (cf Noh & Scalo 1990, and references therein).

Fig. 5 is based on fig. 5 of Pagel (1989). Apart from Pagel's results (crosses), we include (i) our results for the sample corrected for observational errors and cosmic scatter *only* (column 7 of Table 2, empty circles), and (ii) the results corrected also for the scale height effect (column 8 of Table 2 filled circles). Both distributions were also normalized for the total number of stars (132 stars) in Pagel's sample, in order to make the qualitative differences more evident. This corresponds to multiplying the terms within brackets of columns 7 and 8 of Table 2 by 0.46 and 0.41, respectively. Our error bars are similar to those in Pagel's work, and have been omitted from Fig. 5 for the sake of clarity. The figure also shows the predictions of (iii) the simple model with effective yield $p = 0.5\ Z_\odot$, and present gas fraction $\mu_1 = 0.1$; (iv) the simple model with initial production spike, or prompt initial enrichment (PIE); (v) Lynden-Bell's (1975) Best Accretion Model with parameters $M = 20$, $p = Z_\odot$, and $\mu_1 = 0.2$; (vi and (vii) Clayton's (1985, 1988) standard infall models with parameters $k = 2$, $M = 18.5$, $p = 0.75\ Z_\odot$, $\mu_1 = 0.12$, and $k = 4$, $M = 65$, $p = 0.75\ Z_\odot$, and $\mu_1 = 0.12$, respectively. Models (iii)–(vii) are shown as continuous lines labelled in the figure. The analytical formulae and a discussion of the model parameters are given by Pagel (1989). As can be seen from the figure, the simple model does not fit the distribution very well, even at large abundances. The use of differen

© Royal Astronomical Society • Provided by the NASA Astrophysics Data System

1996MNRAS.279..447R

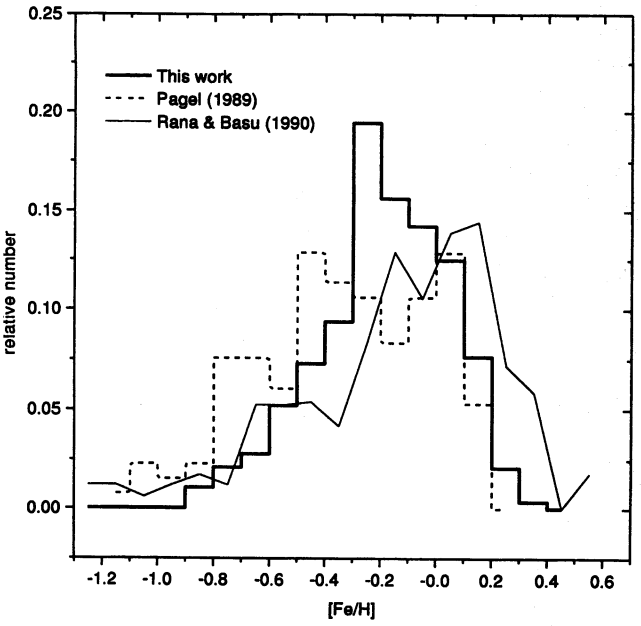

Figure 4. A comparison of our raw metallicity distribution (thick continuous line) and the corresponding quantities from Pagel (1989, broken line) and Rana & Basu (1990, thin line).

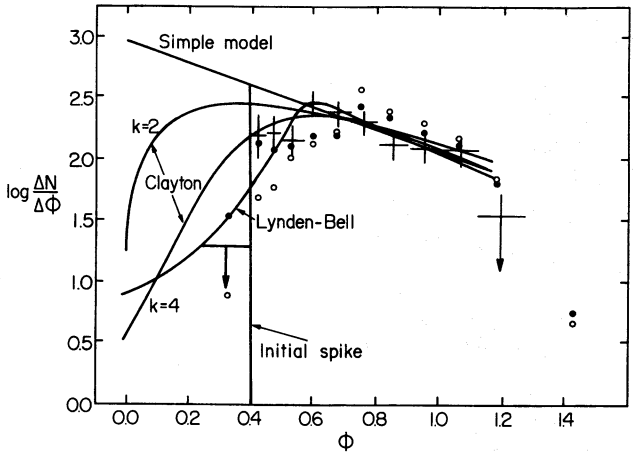

Figure 5. An adaptation of fig. 5 by Pagel (1989) with the inclusion of results of the present work. Filled circles: corrected sample (Table 2, column 8); empty circles: partially corrected sample (Table 2, column 7); crosses: results by Pagel (1989); continuous lines: model fits as given by Pagel (1989).

values for the effective yield does not help this situation. The simple model with an effective yield does not seem to be a good approximation to the chemical evolution of the solar neighbourhood. It can also be seen that infall models tend to decrease the differences between the theoretical and observed distributions.

The G dwarf problem is evident in this plot. The simple model predicts too many metal-poor stars relative to what is found in our vicinity. However, the G dwarf problem may not only be the paucity of metal-poor dwarfs. A smaller number of metal-rich dwarfs is also found relative to the simple model predictions, as shown in Fig. 5. This feature is apparent in some previous metallicity distributions (e.g. Pagel 1989), but

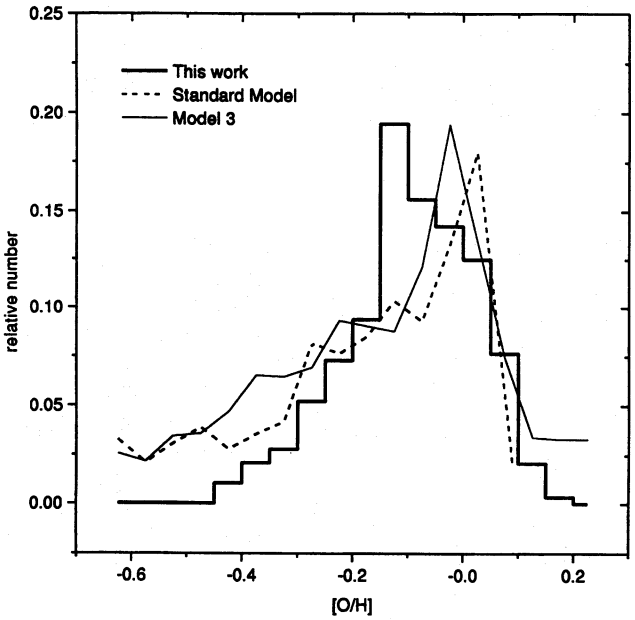

Figure 6. Raw metallicity distribution of G dwarfs (thick continuous line) compared with two chemical evolution models from Giovagnoli & Tosi (1995), corresponding to their standard model (broken line) and model 3 (thin line).

has not been commented upon. The use of a larger star sample, preferably having metallicities obtained by high-resolution spectroscopy, may in the future confirm whether or not this feature is real.

The application of the Sommer-Larsen correction to our sample increases the number of metal-poor stars, and alleviates somewhat the G dwarf problem, but does not completely solve it. On the other hand, the agreement between the data and the model curves, especially Clayton's standard model with $k = 4$, and Lynden-Bell's model, improves very much.

Fig. 6 shows a comparison between our raw metallicity distribution (thick continuous line) and two infall models from the recent work of Giovagnoli & Tosi (1995), corresponding to their standard model (broken line) and model 3 (thin line). Both models use an exponentially decreasing star formation rate with e-folding time $\tau = 15$ Gyr, and a constant infall rate of 4×10^{-3} $M_\odot$ kpc^{-2} yr^{-1}. The main difference between the models is that the standard model uses classic yields from the literature (Díaz & Tosi 1986; Tosi 1988), and Tinsley's (1980) initial mass function, while model 3 uses metallicity-dependent yields given by Maeder (1992), and Salpeter's (1955) initial mass function. The agreement between the data and the models is good, but they still predict an excess of metal-poor stars. The problem could be with a constant infall rate. An infall like that of Lynden-Bell, which rises to a maximum during the lifetime of the Galaxy, and has a smooth decay later on, may produce the small number of metal-poor stars observed, as suggested by Fig. 5. Another possible reason for the observed discrepancy at lower metallicities is that Giovagnoli & Tosi (1995) treat the disc as formed out of metal-free gas, and do not take into account the effect of the halo or the thick disc. If these effects were considered, it could be expected that the disc initial metallicity would be different from zero, and thus fewer metal-poor stars would be produced (Tosi 1995, private communication).

© Royal Astronomical Society • Provided by the NASA Astrophysics Data System

1996MNRAS.279..447R

ACKNOWLEDGMENTS

We thank Gustavo F. Porto de Mello and Cristina Chiappini for some helpful discussions, and Dr B.E.J. Pagel for his comments on an earlier version of this paper. This work was partially supported by CNPq and FAPESP.

NOTE ADDED IN PROOF

After this paper had been submitted for publication, we learned about another determination of the metallicity distribution of G dwarfs by Wyse & Gilmore (1995). Their distribution comprises 128 F and G dwarfs from the catalogue of Gliese & Jahreiss (1991). The stellar metallicities are obtained by the use of the calibration of Schuster & Nissen (1989), also presented in this paper, and photometric data are taken from Olsen (1983). The comparison between their original metallicity distribution (not corrected for the inclusion of stars with lifetime shorter than the Galactic age) and our raw metallicity distribution shows a remarkable agreement.

REFERENCES

Bazan G., Mathews G.J., 1990, ApJ, 354, 644
Beers T.C., Preston G.W., Schectman S.A., 1985, AJ, 90, 2089
Burkert A., Truran J.W., Hensler G., 1992, ApJ, 391, 651
Carigi L., 1994, ApJ, 424, 181
Cayrel de Strobel G., Hauck B., François P., Thévenin F., Friel E., Mermilliod M., Borde S., 1992, A&AS, 95, 273
Clayton D.D., 1985, in Arnett W.D., Truran J.W., eds, Nucleosynthesis: challenges and new developments. Univ. Chicago Press, Chicago, p. 65
Clayton D.D., 1988, MNRAS, 234, 1
Crawford D.L., 1975, AJ, 80, 955
Díaz A.I., Tosi M., 1986, A&A, 158, 60
Duquennoy A., Mayor M., 1991, A&AS, 88, 281
Edvardsson B., Anderson J., Gustafsson B., Lambert D.L., Nissen P.E., Tomkin J., 1993, A&A, 275, 101
Geisler D., Friel E.D., 1992, AJ, 104, 128
Giovagnoli A., Tosi M., 1995, MNRAS, 273, 499
Gliese W., 1969, Veröff Astron. Rechen-Inst. Heidelberg, No. 22
Gliese W., Jahreiss H., 1991, Third Catalogue of Nearby Stars. Astron Rechen-Inst. Heidelberg
Hauck B., Mermilliod M., 1990, A&AS, 86, 107
Kuijken K., Gilmore G., 1989, MNRAS, 239, 571
Laird J.B., Rupen M.P., Carney B.W., Latham D.W., 1988, AJ, 96, 190
Lynden-Bell D., 1975, Vistas Astron. 19, 299
Maeder A., 1992, A&A, 264, 105
Meusinger H., Stecklum B., 1992, A&A, 256, 415
Noh H.-R., Scalo J., 1990, ApJ, 352, 605
Norris J.E., Ryan S.G., 1989, ApJ, 340, 739
Oblak E., 1978, A&AS, 34, 453
Olsen E.H., 1983, A&AS, 54, 55
Olsen E.H., 1984, A&AS, 57, 443
Olsen E.H., 1993, A&AS, 102, 89
Pagel B.E.J., 1987, in Gilmore G., Carswell B., eds, The Galaxy. Reidel Dordrecht, p. 341
Pagel B.E.J., 1989, in Beckman J.E., Pagel B.E.J., eds, Evolutionary Phenomena in Galaxies. Cambridge Univ. Press, Cambridge, p. 201
Pagel B.E.J., Patchett B.E., 1975, MNRAS, 172, 13
Pardi M.C., Ferrini F., 1994, ApJ, 421, 491
Rana N.C., 1991, ARA&A, 29, 129
Rana N.C., Basu S., 1990, Ap&SS, 168, 317
Salpeter E.E., 1955, ApJ, 121, 161
Schmidt M., 1963, ApJ, 137, 758
Schuster W.J., Nissen P.E., 1989, A&A, 221, 65
Sellwood J.A., Sanders R.H., 1988, MNRAS, 233, 611
Sommer-Larsen J., 1991, MNRAS, 249, 368
Sommer-Larsen J., Yoshii Y., 1990, MNRAS, 243, 468
Tinsley B.M., 1980, Fundam. Cosmic. Phys., 5, 287
Tosi M., 1988, A&A, 197, 33
van den Bergh S., 1962, AJ, 67, 486
Woolley R., Epps E.A., Penston M.J., Pocock S.B., 1970, R. Obs. Ann. No. 5
Wyse R.F.G., Gilmore G., 1995, preprint

This paper has been produced using the Royal Astronomica Society/Blackwell Science TEX macros.

© Royal Astronomical Society • Provided by the NASA Astrophysics Data System